Available online at www.sciencedirect.com
ScienceDirect
Journal of Sound and Vibration 323 (2009) 130–147
JOURNAL OF SOUND AND VIBRATION
www.elsevier.com/locate/jsvi

Wavelet analysis for identification of damping ratios and natural frequencies

Shyh-Leh Chen*, Jia-Jung Liu, Hsiu-Chi Lai

Department of Mechanical Engineering, National Chung-Cheng University, Chia-Yi 621, Taiwan, ROC

Received 18 October 2006; received in revised form 1 January 2009; accepted 8 January 2009
Handling Editor: L.G. Tham
Available online 9 March 2009

Abstract

This study addresses the identification of damping ratios and natural frequencies in linear structural dynamic systems. A previously proposed method based on the Morlet wavelet transform of the system's response is investigated analytically. The method can be applied to single- or multi-degree of freedom, lightly or heavily damped systems. It utilizes a relationship between natural frequency, damping ratio and the continuous Morlet wavelet transform of the system response. It is found that the validity of the relationship depends on the scaling factor a, translation factor b, and the frequency parameter ω_0 of the Morlet wavelet transform. A general guideline of choosing a, b, and ω_0 is provided in this paper. Both numerical and experimental results verify the theoretical analysis.

1. Introduction

Parameter identification is a fundamental problem in vibration engineering practice. It is concerned with the estimation of system parameters like natural frequencies and damping ratios. With these parameters, one can obtain the mathematical model for representing a system's input–output relationship. Most existing parameter identification methods are based on the Fourier analysis (see, e.g., Ref. [7]). The Fourier techniques are especially useful in estimating a system's natural frequencies. However, there are several restrictions for the Fourier analysis. First, for noisy data, the spectrum of a signal alone (obtained by FFT) may not provide adequate information for identification. Some de-noising procedure, such as passing through a low-pass filter or notch filter, has to be performed in advance to separate the signal from the noise [15]. Second, for multi-degree-of-freedom (dof) systems with strongly coupled modes, the identification based on the Fourier technique usually cannot give results as good as those for single-dof systems [24]. Finally, the Fourier approach cannot obtain good estimation in damping, especially for heavily damped systems. In particular, for systems with damping ratio greater than $1/\sqrt{2}$, no peaks exist in the spectrum and the Fourier approach fails.

On the other hand, wavelet analysis has gained a great deal of attention in the engineering literature recently due to its excellent capability in signal analysis [3,12,13]. The ability of multi-resolution inherent in the wavelet

*Corresponding author. Tel.: +886 5 242 8262; fax: +886 5 272 0589.
E-mail address: imeslc@ccu.edu.tw (S.-L. Chen).

0022-460X/$ - see front matter © 2009 Elsevier Ltd. All rights reserved.
doi:10.1016/j.jsv.2009.01.029

analysis can automatically filter out the noise from the signal in the process of parameter identification [2,6]. No additional filters are needed. Moreover, the wavelet analysis possesses localization property in both time and frequency domains [2]. Therefore, the frequency resolution of a wavelet transform can be tuned sufficiently small to separate two signals with close frequency contents. This property is useful for identification of multi-dof systems with strongly coupled modes.

Many studies have taken the advantages of wavelet analysis to the problems of system identification. Priebe and Wilson [17] demonstrated that wavelet transform can be used to exploit the time-scale features of structural responses and hence is potentially useful in system identification applications. In general, there are two approaches. The first approach is based on discrete wavelet transform. That is, the system's input and output signals are spanned by wavelet basis functions. The modal parameters can be obtained by the discrete wavelet transform of input and output signals [21]. Robertson et al. [18,19] presented a method of extracting the impulse response from the measured response histories and disturbance of linear structural dynamic systems using discrete wavelet transform. The obtained impulse responses were then utilized for system realizations. From the state-space model, the system's structural modes and damping parameters were estimated. Ghanem and Romeo [4,5] proposed an identification method for linear time-varying systems and nonlinear systems using Daubechies wavelet basis. Chen [1] proposed a Haar wavelet-based identification method for linear time-varying systems. There also exist similar methods for the identification of discrete time models [14,27,28].

The second approach is based on continuous wavelet transform, which was originally proposed by Staszewski and Cooper [23]. Later on, Ruzzene et al. [20] and Staszewski [24] found that there exists a special relationship between modal parameters and the Morlet wavelet transform of the system's impulse response. Hence, the modal parameters can be identified accordingly. The multi-resolution property of wavelet transform was utilized to filter out measurement noise. Furthermore, the localization property of wavelet transform was used to separate different modes in the multi-dof case. The method has been applied to real data from a bridge in Ref. [20] and an aircraft in Ref. [26], and was extended to backbone characteristics in Ref. [25]. Some studies indicated that the Morlet wavelet transform is better than the Hilbert transform or Hilbert–Huang transform in estimating the modal parameters [20,29]. Following the same line, several studies have refined the Morlet wavelet-based identification method to achieve better estimation accuracy [9,11,22,29]. Based on similar analysis with the help of multi-resolution analysis, Lamarque et al. [10] proposed a wavelet-logarithmic decrement method for damping identification in multi-dof systems.

Although the identification method by the Morlet wavelet transform has shown promising results, several issues remain to be studied. First, the method was based on rough approximation using Taylor series expansion. The assumptions leading to the approximation were vague. Consequently, the limitations of the method were not clear. In addition, the identification results depend strongly on the proper choice of scaling factor a, translation factor b, and the frequency parameter ω_0 of the Morlet wavelet transform. Without more accurate derivation, the general guideline of choosing proper a, b, and ω_0 is difficult to obtain. Second, the results of Ruzzene et al. [20] and Staszewski [24] were based on free response. However, the free or impulse response is sometimes not easy to obtain in practice. For example, it is in general difficult, if not impossible, to obtain the free or impulse response for large-scale structural systems such as a bridge. Also, for delicate equipments such as the DVD system, taking impulse response may damage the system. In these cases, forced responses are preferred. Finally, the method was verified only for lightly damped systems. No results on heavily damped systems were presented.

In this work, a more accurate derivation on the Morlet wavelet-based identification method is presented. Based on the accurate derivation, a general guideline of choosing a, b, and ω_0 will be provided. Also, the restrictions of the method will be discussed. It will be shown that the method is actually not restricted to lightly damped systems. Another objective of this work is to generalize the method to allow for the forced response as the source signal. It will be shown that this is possible under certain conditions. In general, the forced response contains the free response (in the transient period). Hence, it can be used for parameter identification. In addition to simulations, the method will also be verified experimentally.

The paper is organized as follows. After the introduction, the identification method for single-dof systems is introduced in Section 2. Both free and forced responses will be discussed. In Section 3, the method is

generalized to multi-dof systems. The method is verified by simulations in Section 4 and by experiments in Section 5. Finally in Section 6, conclusions are drawn.

2. Single degree-of-freedom system

We consider first a linear time-invariant vibration system with one-degree of freedom. The body of mass m is connected by a spring and viscous damper to a fixed support, with a harmonic force of frequency ω and amplitude f_e acting upon it, in the line of motion. The equation of motion is

$$m\ddot{x} + c\dot{x} + kx = F(t) \tag{1}$$

where x is the displacement of the mass m, c is the damping, k is the stiffness and $F(t)$ is the excitation force which is a pure cosine function,

$$F(t) = f_e \cos \omega t \tag{2}$$

Substituting Eq. (2) into (1), and expressing it in terms of natural frequency ω_n and damping ratio ζ, we obtain

$$\ddot{x} + 2\zeta\omega_n\dot{x} + \omega_n^2 x = f \cos \omega t \tag{3}$$

where $f = f_e/m$, $\omega_n{}^2 = k/m$, and $\zeta = c/2\sqrt{mk}$. It is assumed that $0 < \zeta < 1$.

2.1. Identification by free response

The free response (or impulse response) of the system (3) is given by

$$x(t) = A_0 e^{-\zeta\omega_n t} \cos(\omega_d t - \phi_0) \tag{4}$$

where A_0 and ϕ_0 depend on initial condition, and $\omega_d = \omega_n\sqrt{1-\zeta^2}$ is the damped natural frequency. With the system response in hand, the next step is to look for the relations of its Morlet wavelet transform to the system's natural frequency and damping ratio. The Morlet wavelet is defined in the time domain by

$$g(t) = e^{j\omega_0 t} e^{(-1/2)t^2}$$

where ω_0 is a tunable frequency. By setting $\tau = t - b/a$, the Morlet wavelet transformation of the system response (4) can be expressed as

$$W_g x(a,b) = \sqrt{a}\int_{-\infty}^{\infty} x(a\tau + b) g^*(\tau)\, d\tau \tag{5}$$

where a is the scaling factor and b is the translation factor of the Morlet wavelet transform, and the superscript "*" denotes the complex conjugate. Substituting Eq. (4) into (5) and expressing the cosine function in the complex exponential form, one can obtain

$$W_g x(a,b) = \tfrac{1}{2} A_0 \sqrt{a} e^{-\zeta\omega_n b}[I_1 + I_2]$$

where

$$I_1 = \int_{-\infty}^{\infty} e^{-(1/2)\tau^2 - (\zeta\omega_n a + j\omega_0 - j\omega_d a)\tau + j(\omega_d b - \phi_0)}\, d\tau$$

$$I_2 = \int_{-\infty}^{\infty} e^{-(1/2)\tau^2 - (\zeta\omega_n a + j\omega_0 + j\omega_d a)\tau - j(\omega_d b - \phi_0)}\, d\tau$$

By completing the square on the exponential argument, I_1 can be rewritten as

$$I_1 = e^{j(\omega_d b - \phi_0) + (1/2)(\zeta\omega_n a + j\omega_0 - j\omega_d a)^2} \int_{-\infty}^{\infty} e^{-(1/2)[\tau + (\zeta\omega_n a + j\omega_0 - j\omega_d a)]^2}\, d\tau \tag{6}$$

Similarly, I_2 can be rewritten as

$$I_2 = e^{-j(\omega_d b-\phi_0)+(1/2)(\zeta\omega_n a+j\omega_0+j\omega_d a)^2}\int_{-\infty}^{\infty} e^{-(1/2)[\tau+(\zeta\omega_n a+j\omega_0-j\omega_d a)]^2}\,d\tau \tag{7}$$

By the method of contour integral, it is shown in appendix that $\forall\alpha\in\Re,\beta\in\Re$,

$$\int_{-\infty}^{\infty} e^{(-1/2)(\tau+\alpha+j\beta)^2}\,d\tau = \sqrt{2\pi} \tag{8}$$

It implies that both integrals in Eqs. (6) and (7) are equal to $\sqrt{2\pi}$. Hence, we have

$$\begin{aligned} W_g x(a,b) &= \frac{\sqrt{2\pi a}}{2}A_0 e^{-\zeta\omega_n b}\left[e^{j(\omega_d b-\phi_0)+(1/2)(\zeta\omega_n a+j\omega_0-j\omega_d a)^2}+e^{-j(\omega_d b-\phi_0)+(1/2)(\zeta\omega_n a+j\omega_0+j\omega_d a)^2}\right]\\ &= \frac{\sqrt{2\pi a}}{2}A_0 e^{-\zeta\omega_n b-(1/2)[(1-2\zeta^2)\omega_n^2 a^2+\omega_0^2]+j\zeta\omega_0\omega_n a}(e^{\theta}+e^{-\theta}) \end{aligned}$$

where

$$\theta = \omega_0\omega_d a + j(\omega_d b-\phi_0) - j\zeta\omega_n\omega_d a^2$$

Assume that

$$\omega_0\omega_d a \gg 1 \tag{9}$$

By taking ω_0 large enough, this assumption can be easily satisfied. Assumption (9) implies that $|e^{-\theta}|\ll|e^{\theta}|$, and $W_g x(a, b)$ can be approximated by

$$W_g x(a,b) \approx \frac{\sqrt{2\pi a}}{2}A_0 e^{\alpha+j\beta} \tag{10}$$

where

$$\begin{aligned} \alpha &= -\zeta\omega_n b - \tfrac{1}{2}[(1-2\zeta^2)\omega_n^2 a^2 - 2\omega_0\omega_d a+\omega_0^2]\\ \beta &= \omega_d b-\phi_0+\zeta\omega_0\omega_n a-\zeta\omega_n\omega_d a^2 \end{aligned}$$

Therefore, fixing the scaling factor, i.e., taking $a = a_0$, one can obtain

$$\ln|W_g x(a_0,b)| \approx -\zeta\omega_n b + c_1 \tag{11}$$

$$\angle W_g x(a_0,b) \approx \omega_d b + c_2 \tag{12}$$

where c_1 and c_2 are independent of the translation factor b, and are given by

$$\begin{aligned} c_1 &= -\frac{1}{2}[(1-2\zeta^2)\omega_n^2 a_0^2 - 2\omega_0\omega_d a_0+\omega_0^2]+\ln\frac{\sqrt{2\pi a_0}A_0}{2}\\ c_2 &= -\phi_0+\zeta\omega_0\omega_n a-\zeta\omega_n\omega_d a^2 \end{aligned}$$

It is now obvious that damping ratio ζ and natural frequency ω_n can be estimated, respectively, from the slopes of the logarithm of modulus and phase of the wavelet transform with respect to parameter b. That is,

$$\text{slope of } \ln|W_g x(a_0,b)| \quad \text{v.s.} \quad b = -\zeta\omega_n \tag{13}$$

$$\text{slope of } \angle W_g x(a_0,b) \quad \text{v.s.} \quad b = \omega_n\sqrt{1-\zeta^2} \tag{14}$$

These two equations will yield ζ and ω_n.

Theoretically, the relationships given by Eqs. (13) and (14) hold for any fixed a_0 and any range of b. However, one should note that in general the free response given in Eq. (4) is valid only for positive time, and $x(t) = 0$, $\forall t<0$. Note also that for given a and b, the wavelet transform works as a window function in both time and frequency domains [2]. The scaling factor a determines the frequency window and the time window

depends on both a and b. Hence, the derivation is not valid for b being too small (where the time window covers the negative time zone). This phenomenon is usually referred to as the end effect [8]. Also in practice, the response signal is usually contaminated with noise or numerical errors, which will affect the results. In other words, the wavelet transform of a practical response should be given by

$$W_g\tilde{x}(a,b) = W_g x(a,b) + W_g x_n(a,b)$$

where $\tilde{x}(t)$ represents the practical response and $x_n(t)$ is the noise. Better results can be obtained by properly choosing a_0 and b to satisfy

$$|W_g x_n(a_0,b)| \ll |W_g x(a_0,b)| \tag{15}$$

That is, the contribution from noises is negligible.

The above derivations and discussions show that the validity of Eqs. (13) and (14) depends on the scaling factor a, translation factor b, and the frequency parameter ω_0 of the Morlet wavelet transform. To yield good identification results, proper choice of ω_0, a_0 and b is necessary. A general guideline of choosing these parameters is provided below.

- ω_0 is taken large enough so that Eq. (9) holds.
- a_0 is taken at the peak of $|W_g x(a, b)|$. The spectrum of the free response will reach a peak in a neighborhood of the natural frequency. This peak will correspond to that of the wavelet transform. Hence, the frequency window associated with the choice a_0 will cover the neighborhood of the natural frequency. As a result, when the noise is separated from the natural frequency, it can be automatically filtered out by the frequency window.
- b is taken in the range of positive small values where the log-magnitude plot becomes linear with a negative slope. The time window with this range of b will cover the transient period and the positive time zone. It is the transient response that contains the information of modal parameters. As one can see from Eq. (10), $W_g x(a, b)$ decreases exponentially with the increase in b. Positive small values of b will also make (15) be easily satisfied. On the other hand, b should not be taken too small; otherwise, the time window will cover too much of the negative time zone, where the end effect takes place [8,9].

Finally, some remarks on the damping ratio are made. Most similar approaches assumed low damping ratios [20,24]. A lightly damped system possesses the property that the system's frequency response is highly localized in a neighborhood of the natural frequency. It is this property that makes proper a_0 and b be easily chosen so that the associated frequency and time windows can cover the regions with necessary modal information. For systems with wide band frequency response, it is more difficult to choose a_0 and b. As one can see from Eq. (10), if $\zeta \geqslant 1/\sqrt{2}$, then $|W_g x(a, b)|$ increases with a and no peak exists.

Theoretically, the proposed approach does not respect the size of damping ratio, as implied by Eqs. (11)–(14). The assumption of low damping ratios is in fact not necessary here. The only assumption is (9). However, for heavily damped systems, ω_d is small and hence ω_o should be taken larger so that Eq. (9) still holds. Moreover, large damping ratios may cause large estimation errors due to numerical errors or external noises. It should be noted that $e^{-\zeta\omega_n b}$ is smaller with larger ζ, making the contribution of numerical errors or external noises relatively important. In this case, b should be taken smaller. Also, a_o should be taken smaller so that the frequency window is larger to cover the wide band frequency response. On the other hand, if a_o is taken too small, then α in Eq. (10) is small and again, Eq. (15) may not hold. It is concluded that more delicate choice of a_o and b is necessary for heavily damped systems. In general, large ω_o, positive small values of a_o and b should be taken.

2.2. Identification by forced response

The task of identification is to provide proper excitation inputs to the system such as impulse, step, or harmonic signal. The resulting output responses are then utilized to estimate the system parameters. Since impulse or free responses contain complete system information, they are used in most identification schemes. However, generating impulse or free responses is difficult or improper in some cases. In these cases, one can

provide the system with proper forcing excitation instead. Here, it is assumed that the provided excitation is a harmonic input given by Eq. (2). Note that in parameter identification, one usually has the authority to control the input signal. If, unfortunately, the excitation inputs are not what we can control, the proposed method may fail.

The forced response of Eq. (3) includes homogeneous and particular parts. The homogeneous solution represents the contribution from the initial condition that quickly dies away, i.e., the free response given in Eq. (4). The sustained motion is given by the particular solution, which is given by

$$x_p = A\cos(\omega t - \phi)$$

where

$$A = \frac{f}{[(2\zeta\omega\omega_n)^2 + (\omega_n^2 - \omega^2)^2]^{1/2}} \quad \text{and} \quad \phi = \tan^{-1}\frac{2\zeta\omega_n\omega}{\omega_n^2 - \omega^2}$$

The complete solution to Eq. (3) is

$$x(t) = x_h(t) + x_p(t) \tag{16}$$

where x_h represents the free response given by Eq. (4). Since the wavelet transform is linear, the wavelet transform of homogeneous (denoted by $W_g x_h(a, b)$) and particular ($W_g x_p(a, b)$) solutions can be computed separately. The former has been obtained in Eq. (10). Consider $W_g x_p(a, b)$ now. Following the same line presented in Section 2.1 for $W_g x_h(a, b)$, one can obtain

$$W_g x_p(a,b) = \frac{\sqrt{2\pi a}}{2} A e^{-(1/2)\omega_0^2 - (1/2)(\omega a)^2}[e^{\omega_0\omega a + j(\omega b - \phi)} + e^{-\omega_0\omega a - j(\omega b - \phi)}] \tag{17}$$

Assume that

$$\omega_0\omega a \gg 1 \tag{18}$$

which can be satisfied by taking ω_0 large enough. Then

$$|e^{-\omega_0\omega a - j(\omega b - \phi)}| \ll |e^{\omega_0\omega a + j(\omega b - \phi)}|$$

and Eq. (17) can be approximated by

$$W_g x_p(a,b) \approx \frac{\sqrt{2\pi a}}{2} A e^{\gamma + j\delta}$$

where

$$\gamma = -\tfrac{1}{2}\omega^2 a^2 + \omega_0\omega a - \tfrac{1}{2}\omega_0^2$$
$$\delta = \omega b - \phi$$

Thus, under assumptions (9) and (18) the Morlet wavelet transform of the forced response can be approximated by

$$W_g x(a,b) = W_g x_h(a,b) + W_g x_p(a,b) = \frac{\sqrt{2\pi a}}{2}[A_0 e^{\alpha + j\beta} + A e^{\gamma + j\delta}] \tag{19}$$

where recall that the homogenous part is given by Eq. (10).

In what follows, we shall show that

$$|W_g x_p(a,b)| \ll |W_g x_h(a,b)| \tag{20}$$

if ω_0 is sufficiently large and the forcing frequency is small enough so that

$$\omega < \omega_d \tag{21}$$

To this aim, note that by Eq. (19)

$$\frac{|W_g x_p(a,b)|}{|W_g x_h(a,b)|} \approx \frac{A}{A_0} e^{\gamma - \alpha} \tag{22}$$

In general, A_0 is of the same order as A. The most common situation in practice is zero initial conditions. Under zero initial conditions, it can be shown that if assumption (21) holds, then

$$\frac{A}{A_0} \approx \sqrt{1-\zeta^2}$$

which implies that A_0 and A are of the same order. Next, we compute

$$\gamma - \alpha = -\omega_0 a(\omega_d - \omega) + \tfrac{1}{2}(1-2\zeta^2)\omega_n^2 a^2 - \tfrac{1}{2}\omega^2 a^2 + \zeta\omega_n b \tag{23}$$

Under assumption (21), ω_0 can be chosen sufficiently large so that

$$\gamma - \alpha \ll 0 \tag{24}$$

which implies (20).

Assumptions (9), (18), and (21) can be combined as

$$1 \ll \omega_0 \omega a < \omega_0 \omega_d a \tag{25}$$

With assumption (25), the Morlet wavelet transform of the forced response can be approximated by that of the free response, i.e., $W_g x(a, b) \approx W_g x_h(a, b)$. Thus, the results for the free response also hold for the forced response. In other words, it is still the transient response that is utilized for identification. As mentioned previously, if the forcing term cannot be controlled, the forcing frequency may be close to the natural frequency and inequality (25) does not satisfy. Then, the proposed method will fail.

3. Multi-degree-of-freedom system

In this section, the parameter identification method proposed in the previous section will be generalized to multi-degree-of-freedom systems. Without loss of generality, the free response of a 2-dof system is taken as an illustrative example here. The extension to general multi-dof systems is straightforward. Let ζ_i and ω_{ni} be the damping ratio and natural frequency of the ith mode. The response of a 2-dof system can be expressed as the sum of the contributions from 2 modes, i.e.,

$$x(t) = x_1(t) + x_2(t) \tag{26}$$

where

$$x_i(t) = A_i e^{-\zeta_i \omega_{ni} t} \cos(\sqrt{1-\zeta_i^2}\omega_{ni} t - \phi_i), \quad i = 1, 2$$

denotes the contribution from the ith mode. Again, A_i and ϕ_i are determined by the initial conditions. If the initial conditions can be chosen so that $A_1 \neq 0$ and $A_2 = 0$, then the problem is reduced to the case of 1-dof. In other words, only one mode is excited by proper initial condition, and the associated modal parameters can be identified. In practice, however, it is very difficult to place the initial conditions on a specific mode shape. Therefore, the system response usually contains the information from all modes, such as (26). The wavelet transform is thus given by

$$W_g x(a,b) = W_g x_1(a,b) + W_g x_2(a,b) = \frac{\sqrt{2\pi a}}{2}\left[A_1 e^{\alpha_1 + j\beta_1} + A_2 e^{\alpha_2 + j\beta_2}\right]$$

where

$$\alpha_i = -\zeta_i \omega_{ni} b - \frac{1}{2}\left[(1-2\zeta_i^2)\omega_{ni}^2 a^2 - 2\omega_0\sqrt{1-\zeta_i^2}\omega_{ni} a + \omega_0^2\right]$$

$$\beta_i = \sqrt{1-\zeta_i^2}\omega_{ni} b - \phi_i + \zeta_i \omega_o \omega_{ni} a - \zeta_i \sqrt{1-\zeta_i^2}\omega_{ni}^2 a^2$$

Again, the localization property of wavelet transform is utilized to identify the modal parameters of each mode. The idea is to choose a proper scaling factor a_1 so that the frequency window covers only the first mode, and filter out the second mode. In other words,

$$|W_g x_1(a_1, b)| \gg |W_g x_2(a_1, b)| \tag{27}$$

Another scaling factor a_2 can be chosen so that

$$|W_g x_2(a_2, b)| \gg |W_g x_1(a_2, b)| \tag{28}$$

To this aim, it is assumed that

$$\zeta_i < \frac{1}{\sqrt{2}} \tag{29}$$

Recall that if $\zeta_i \geqslant (1/\sqrt{2})$, then $|W_g x_i(a, b)|$ does not have any peaks, and the two modes will be strongly coupled. In this case, both modes have important contribution to $W_g x(a, b)$. Separating the two modes becomes very difficult.

With assumption (29), both $|W_g x_1(a, b)|$and $|W_g x_2(a, b)|$ possess a peak. The peak of $|W_g x_1(a, b)|$ can be approximated by that of e^{α_1}, which occurs at

$$a_1 = \frac{\sqrt{1-\zeta_1^2}\omega_0}{(1-2\zeta_1^2)\omega_{n1}}$$

Similarly, the peak of $|W_g x_2(a, b)|$ occurs approximately at

$$a_2 = \frac{\sqrt{1-\zeta_2^2}\omega_0}{(1-2\zeta_2^2)\omega_{n2}}$$

At $a = a_1$, we have

$$|W_g x_1(a_1, b)| = \frac{\sqrt{2\pi a_1}A_1}{2} e^{-\zeta_1\omega_{n1}b + r_1\omega_0^2} \tag{30}$$

$$|W_g x_2(a_1, b)| = \frac{\sqrt{2\pi a_1}A_2}{2} e^{-\zeta_2\omega_{n2}b + (r_1+r_2)\omega_0^2} \tag{31}$$

where

$$r_1 = \frac{\zeta_1^2}{2(1-2\zeta_1^2)}$$

$$r_2 = \frac{(\zeta_2^2-\zeta_1^2)\omega_r^2}{2(1-2\zeta_1^2)^2} - \frac{\left(\sqrt{1-\zeta_2^2}\omega_r - \sqrt{1-\zeta_1^2}\right)^2}{2(1-2\zeta_1^2)}$$

and $\omega_r = \omega_{n2}/\omega_{n1} > 1$ is the ratio of the two natural frequencies. On the other hand, at $a = a_2$, we have

$$|W_g x_1(a_2, b)| = \frac{\sqrt{2\pi a_2}A_1}{2} e^{-\zeta_1\omega_{n1}b + (r_3+r_4)\omega_0^2} \tag{32}$$

$$|W_g x_2(a_2, b)| = \frac{\sqrt{2\pi a_2}A_2}{2} e^{-\zeta_2\omega_{n2}b + r_3\omega_0^2} \tag{33}$$

where

$$r_3 = \frac{\zeta_2^2}{2(1-2\zeta_2^2)}$$

$$r_4 = \frac{(\zeta_1^2-\zeta_2^2)}{2(1-2\zeta_2^2)^2\omega_r^2} - \frac{\left(\sqrt{1-\zeta_1^2}\omega_r - \sqrt{1-\zeta_2^2}\right)^2}{2(1-2\zeta_2^2)\omega_r^2}$$

From Eqs. (30)–(33), it is obvious that if $r_2 < 0$ and $r_4 < 0$, the mode separation conditions (27) and (28) can be achieved by taking ω_0 large enough. Larger ω_0 implies better frequency resolution and hence close frequencies can still be distinguished. Thus, with large ω_0 mode separation is still possible for close modes.

However, if the two modes are too close, they cannot be separated even with large ω_0. The question is how close is too close? When ζ_i are not small and ω_r is close to 1, either r_2 or r_4 will be positive. As a result, either Eq. (27) or Eq. (28) does not hold. It is concluded that the two modes are too close when either $r_2 \geqslant 0$ or $r_4 \geqslant 0$. Fortunately, this situation is rare. As one can see, either r_2 or r_4 must be negative. Also, $r_2 < 0$ and $r_4 < 0$ can be easily satisfied if ζ_i are small enough (lightly damped systems) or ω_r is large enough (weakly coupled modes). Under conditions (27) and (28), the identification method presented for 1-dof system can be directly applied to $W_g x(a_1, b)$and $W_g x(a_2, b)$ to obtain modal parameters of the first and second modes, respectively. The above results will be verified by an example close-mode system in the next section.

4. Simulation results

Five examples are investigated numerically to verify the theoretical analysis. Examples 1–3 are 1-dof as shown in Fig. 1. For example 1, the system parameters are $m = 1\,\text{kg}$, $c = 0.7\,\text{N s/m}$, $k = 7000\,\text{N/m}$, and they are $m = 1\,\text{kg}$, $c = 15\,\text{Ns/m}$, $k = 70\,\text{N/m}$ for example 2. Example 1 is lightly damped ($\zeta < 1/\sqrt{2}$) and example 2 is heavily damped ($\zeta > 1/\sqrt{2}$). The Morlet wavelet transform (with $\omega_0 = 10$) of a free response of example 1 is shown in Fig. 2. There is a peak at $a_0 = 25$. The corresponding magnitude and phase are plotted in Fig. 3. As one can see, there exists a linear relationship for $b \in [1, 4]$ (positive small values). By curve fitting with least-squares algorithm, one can get the slopes of magnitude and phase. Then, ω_n and ζ can be easily estimated from Eqs. (13) and (14). On the other hand, since example 2 is heavily damped, ω_0 is taken larger. Here we choose $\omega_0 = 20$. Fig. 4 is the Morlet wavelet transform of a free response of example 2. Clearly, there is no peak. By the remarks at the end of Section 2.1, we take $a_0 = 4$, a small value. In fact, other choices of a_0 (not too large, e.g., less than 12) can yield similar results. The magnitude and phase plots with $a_0 = 4$ are presented in Fig. 5. Again, by the remarks at the end of Section 2.1, b is taken in the range of positive small values, i.e., $b \in [0.54, 0.72]$, which is smaller than that for example 1. Finally, the slopes of magnitude and phase can be obtained by curve fitting and ω_n and ζ can be estimated accordingly.

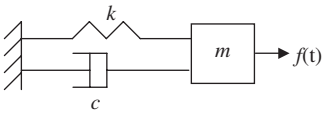

Fig. 1. The single-dof system for examples 1–3.

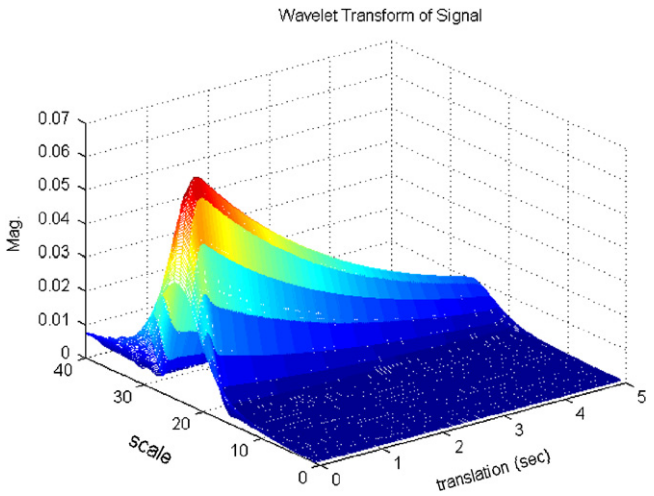

Fig. 2. The Morlet wavelet transform of free response for example 1.

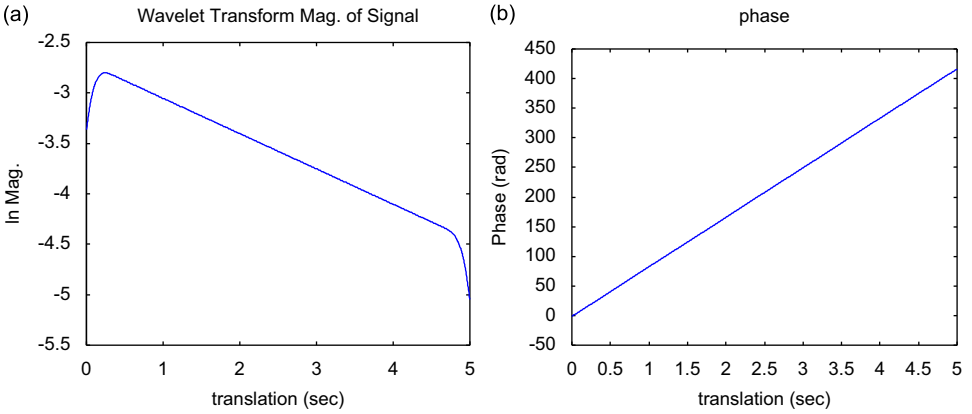

Fig. 3. (a) Magnitude plot and (b) phase plot for example 1 with $a_0 = 25$.

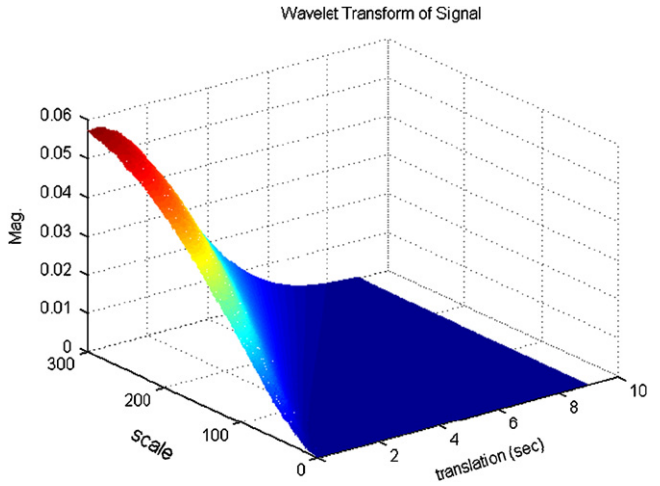

Fig. 4. The Morlet wavelet transform of free response for example 2.

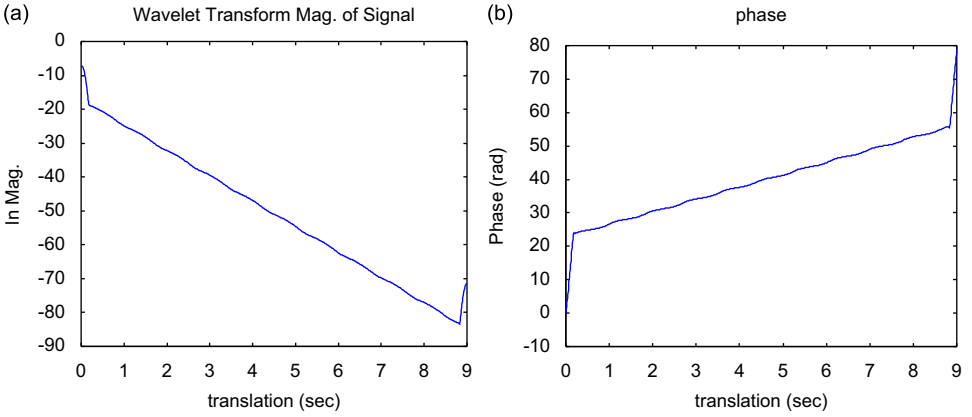

Fig. 5. (a) Magnitude plot and (b) phase plot for example 2 with $a_0 = 4$.

Table 1
Simulation results for 1-dof systems.

Response	ω_0	a_0	Range of b	ω_n (rad/s)	$\hat{\omega}_n$ (rad/s)	Error in $\hat{\omega}_n$ (%)	ζ	$\hat{\zeta}$	Error in $\hat{\zeta}$ (%)
Example 1									
Free	10	25	[1,4]	83.67	83.6660	0.0002	0.00418	0.0042	0.0832
Forced $f(t) = 5\cos(t)$	10	23	[1,4]	83.67	83.6661	0.0002	0.00418	0.0042	0.0749
Example 2									
Free	20	4	[054,0.72]	8.366	8.4343	0.8159	0.8969	0.9607	7.1108
Forced $f(t) = 0.1\cos(0.1t)$	20	4	[0.36, 0.63]	8.366	8.3135	−0.6276	0.8969	0.9569	6.6843
Example 3									
50 s of free response data	5	1000	[20,40]	0.5	0.5013	0.2655	0.1	0.1007	0.6763
15 s of free response data	5	1000	[11,15]	0.5	0.5037	0.7356	0.1	0.1031	3.1069

The estimation results, including the results by forced responses, for examples 1 and 2 are summarized in Table 1. In the following tables, ω_n and ζ denote the actual natural frequency and damping ratio, whereas $\hat{\omega}_n$ and $\hat{\zeta}$ represent the corresponding estimations. For forced responses, the external excitation for example 1 is $5\cos t$, and that for example 2 is $0.1\cos 0.1t$. Recall that the excitation frequency should be less than the damped natural frequency (condition (21)). Thus, the excitation frequency has to be relatively small for heavily damped systems. Table 1 indicates that the identification results for example 1 are quite satisfactory. The estimation errors for both natural frequency and damping ratio using either free or forced responses are all less than 0.1%. This is due to the good localization property of lightly damped systems, as mentioned in Section 2. Because of the wide band frequency response of heavily damped systems, the identification results for example 2 are not as good as those for example 1. However, the estimation error for natural frequency can be kept less than 1%, and that for damping ratio can be kept less than 10%. Again, the results do not respect free or forced responses.

Example 3 is a 1-dof system with system parameters of $m = 1$ kg, $c = 0.1$ N s/m, $k = 0.25$ N/m. It possesses very low natural frequency ($\omega_n = 0.5$ rad/s and $\zeta = 0.1$) and very large settling time (2% settling time is 80 s). The identification results are also shown in Table 1. The corresponding magnitude and phase plots are omitted for brevity. If 50 s of data are used, the estimation accuracy for both ω_n and ζ is as good as that for high-frequency systems. If the data is more limited (e.g., 15 s), the estimation for ω_n has the same level of accuracy. Although the result for ζ is not as good as that for ω_n, it is still reasonable (error about 3%). Note that for systems with low natural frequency, a_0 is usually large (1000 in example 3) and hence b should be taken larger in order not to cover too much of the negative time zone to avoid the edge effect. However, large b will make the corresponding time window cover the portion where the data are cut-off (another edge effect). In this case, a better range of b is around the tail of the data. For example, if the data are 15 s, b is around 11–15.

Example 4 is a 4-dof system as shown in Fig. 6. It has been previously studied in Ref. [20]. Since the damping ratios for all modes are small, better identification results are expected by choosing large enough ω_0. Here we take $\omega_0 = 35$. The Morlet wavelet transform of the impulse response (which is not shown for brevity) possesses 4 peaks. The scaling factors for the 4 modes are taken at these peaks, which are

$$a_1 = 64, \quad a_2 = 34, \quad a_3 = 23, \quad a_4 = 20$$

The impulse response is the displacement response of each mass by assuming an impulse force applied at mass 1. The displacement responses of all masses can be used for identification. Table 2 is the average identification results using the 4 displacement responses. It is concluded that the present approach can be equally applied to multi-dof systems with the same level of accuracy. The estimation errors obtained in Ref. [20] are also provided for comparison. It is clear that the present results are better than those in Ref. [20]. This is because no rules of choosing a and b are provided in Ref. [20]. It is believed that a better set of a and b is taken in this paper.

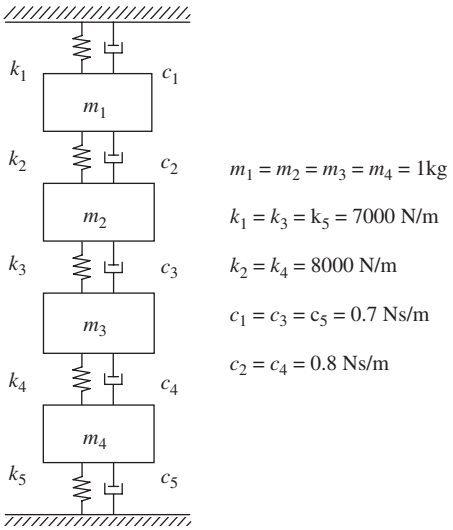

Fig. 6. Schematic diagram of example 4.

Table 2
Simulation results for multi-dof systems.

Mode	a_i	Range of b	ω_n (rad/s)	$\hat{\omega}_n$ (rad/s)	Error in $\hat{\omega}_n$ (%)	Error in $\hat{\omega}_n$ (%) by [20]	ζ (%)	$\hat{\zeta}$ (%)	Error in $\hat{\zeta}$ (%)	Error in $\hat{\zeta}$ (%) by [20]
Example 4										
1	64	[1.8,2.7]	52.5904	52.6099	0.0373	0.12	0.26	0.26	0.811	0
2	34	[0.9, 1.8]	98.8345	98.8326	−0.0019	0.06	0.49	0.49	0.855	2.04
3	23	[0.9, 1.8]	142.5026	142.2502	−0.1772	−0.61	0.71	0.71	0.450	1.40
4	20	[0.9, 1.8]	164.9964	165.0494	0.0321	−8.56	0.83	0.83	−0.308	7.22
Example 5										
1	1008	[3,4]	50.0922	50.0157	−0.1529	N/A	3.07	2.97	−3.145	N/A
2	915	[3,4]	53.7525	54.0553	0.5634		4.40	4.20	−4.592	

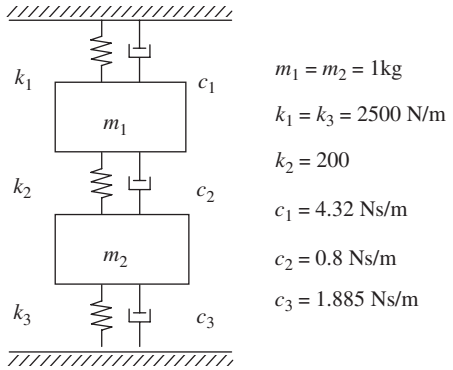

Fig. 7. Schematic diagram of example 5.

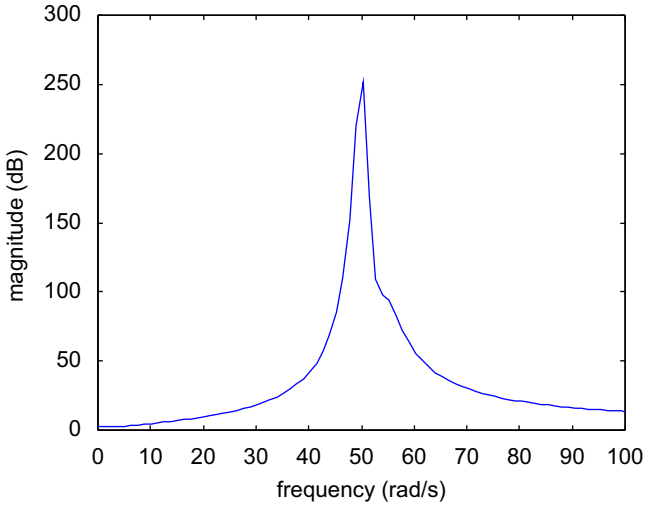

Fig. 8. FFT of free response of example 5.

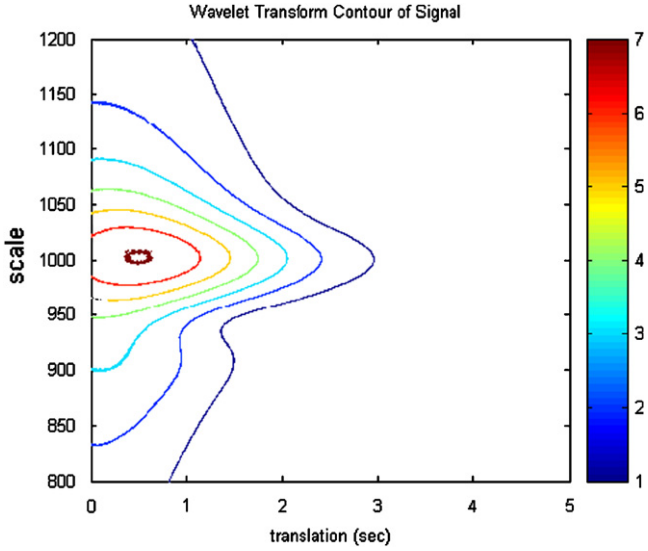

Fig. 9. Contour plot of the Morlet wavelet transform for example 5 with $\omega_0 = 50$.

Example 5 is a 2-dof system, as shown in Fig. 7. The fast Fourier transform (FFT) of a free response shown in Fig. 8 clearly demonstrates that the two modes are strongly coupled. From the system parameters, one can get that the ratio of natural frequencies is $\omega_r = 1.073$, confirming that the two modes are very close. However, theoretical analysis shows that $r_2 = -0.0021$ and $r_4 = -0.0027$, both negative, implying that separation of the two modes is possible by tuning ω_0 large enough. Indeed, the contour plot of the Morlet wavelet transform with $\omega_0 = 50$, i.e., Fig. 9, shows two peaks. The identification results are also presented in Table 2. Although the results are not as good as the case with well-separated modes, the errors for ω_n are less than 1% and those for ζ are less than 5%.

Below are some comments on the simulation results. First, the end effects due to the finite length of data, commonly encountered in wavelet transform [8,9], also appear here, see, e.g., Figs. 3 and 5. This is the reason why the translation factor b cannot be taken too small. Second, in calculating the phase angle of the wavelet transform, one needs to unwrap the phase so that Eq. (12) (and hence Eq. (14)) is satisfied. Finally, it is sometimes difficult to visually identify the peaks (to obtain a_i) from the wavelet plot, especially for the case of

close modes (e.g., in Fig. 9). However, they can be easily obtained by numerically finding the maximum from the wavelet transformed data. On the other hand, the peaks may be easier to be identified using the technique of reassigned wavelets [16]. We shall not pursue the issue here, but leave it as a future work.

5. Experimental results

The validity and feasibility of the proposed method are now examined experimentally. Consider a mass–spring vibration model, which is shown in Fig. 10. The two masses are square steel plates with the same size of 80 mm × 80 mm, and $m_1 = 0.581$ kg, $m_2 = 0.612$ kg. There are 4 holes at the corners on each plate, and 4 vertical beams are used to constrain the mass motion along the vertical direction. Two identical springs ($k_1 = 2686$ N/m) are placed on the diagonal positions between m_1 and base. Hence, the effective spring constant is $2k_1$. Similarly, two identical springs ($k_2 = 7050$ N/m) are placed between m_1 and m_2 with an effective spring constant of $2k_2$. An accelerometer (B&K type 4391) is attached to m_1 to measure the impulse response of m_1. Two examples, one single-dof and one 2-dof, are investigated. The associated parameters are listed in Table 3, where the actual damping is unknown. For the single-dof case, only the lower level of the

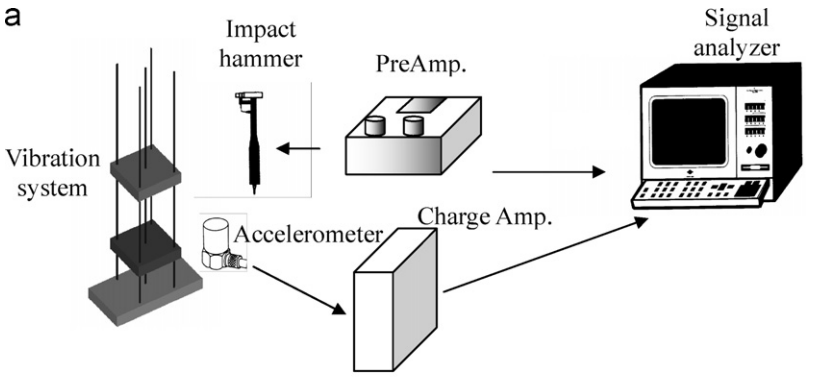

Fig. 10. Experimental set-up: (a) configuration of the experimental set-up and (b) photo of the vibration system.

Table 3
Experimental results.

	ω_0	a_0	Range of b	ω_n (rad/s)	$\hat{\omega}_n$ (rad/s)	Error in $\hat{\omega}_n$ (%)	ζ	$\hat{\zeta}$ (%)
Example 6								
Wavelet	5	56	[0.2, 0.5]	96.205	93.6369	−2.6694	N/A	1.6
Fourier	N/A			96.205	87.96	−8.5702	N/A	4.2
Example 7								
Mode 1								
Wavelet	5	80	[0.25, 0.45]	63.767	64.3192	0.866	N/A	9.71
Fourier	N/A			63.767	65.973	3.4595	N/A	15.2
Mode 2								
Wavelet	5	26.5	[0.1, 0.3]	229.2895	225.7683	−1.536	N/A	3.97
Fourier	N/A			229.2895	223.053	−2.7199	N/A	4.97

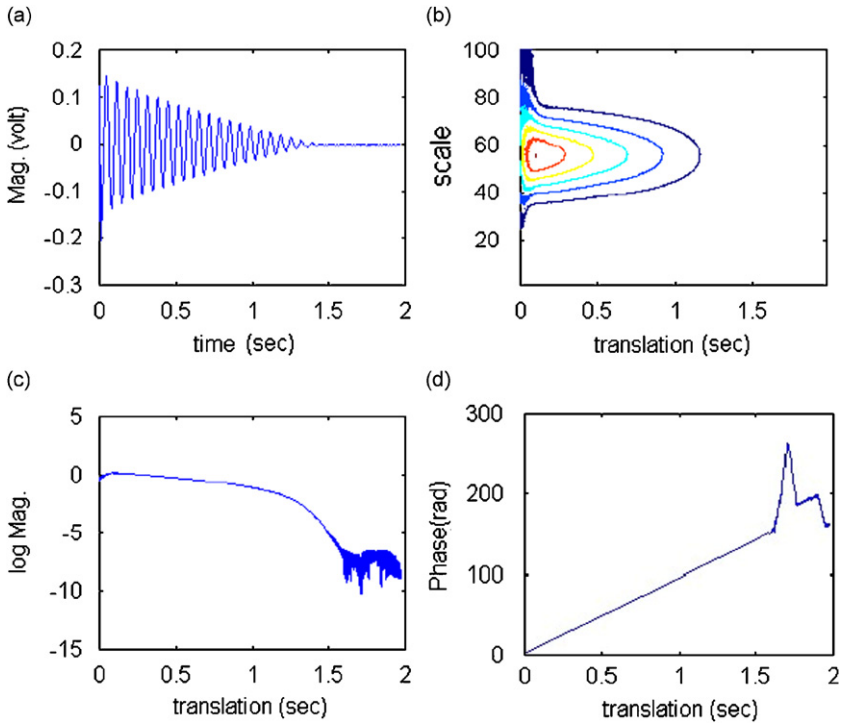

Fig. 11. The Morlet wavelet transform for example 6: (a) impulse response; (b) wavelet transform contour; (c) magnitude plot and (d) phase plot.

experiment is used, i.e., m_2 and $2k_2$ are removed. An impact hammer gives a vertical impulse force on m_1 for the single-dof case and on m_2 for the 2-dof case. The recorded vibration signals are denoised by a signal analyzer (B&K type 2035). The FFT of the denoised signal can thus be obtained by the analyzer, which is used for identification by the Fourier approach. At the same time, the signal (un-denoised) is also used for identification by the proposed Morlet wavelet method. The signal-to-noise ratio is about 20 dB.

Fig. 11 shows the magnitude and phase plots of the Morlet wavelet transform of the impulse response for example 6 with $a_0 = 56$. The natural frequency and damping ratio for example 6 can now be identified with the proposed approach. Similarly, the magnitude and phase plots for the second mode of example 7 are shown in Fig. 12. Those for the first mode are omitted for brevity. The two scales ($a_1 = 80$ and $a_2 = 26.5$) are taken

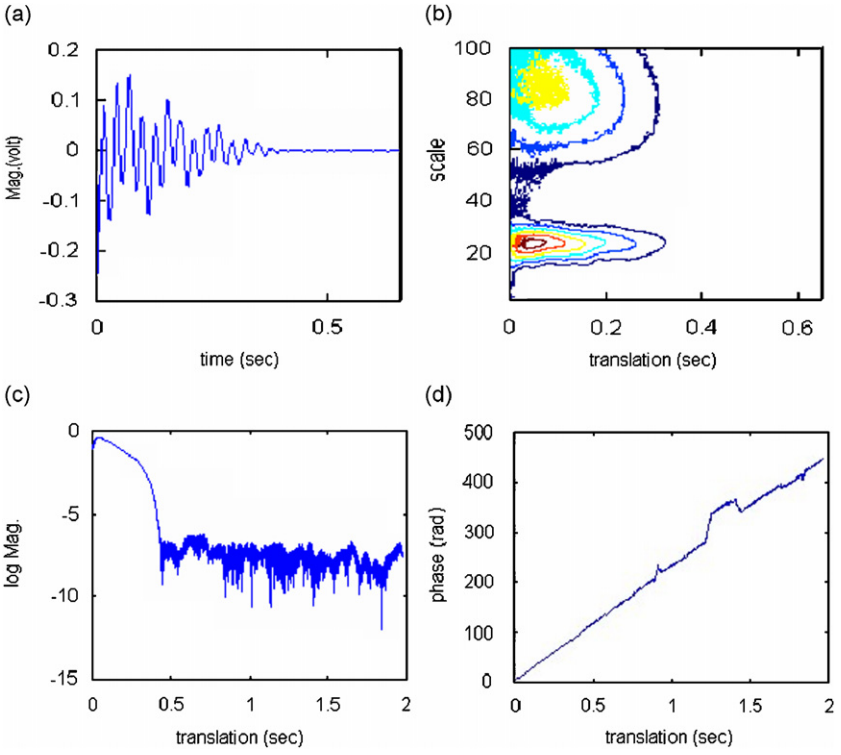

Fig. 12. The Morlet wavelet transform for example 7: (a) impulse response; (b) wavelet transform contour; (c) magnitude plot of 2nd mode and (d) phase plot of 2nd mode.

where the Morlet wavelet transform attains local maximum in magnitude. The estimation results for the two examples are shown in Table 3. Each estimate is the average of 15 times of experiments. From Table 3, one can see that all of the identification errors by the proposed method are within 3%. Also, the results for the 2-dof system are as good as those for the 1-dof system. Note that when b is large, the wavelet plots do not exhibit a linear trend, as can be easily seen from Figs. 12(c) and 13(c). This is due to the fact that $W_g x(a, b)$ decreases exponentially with the increase of b. Thus, the contribution from noise, that is present in the experimental data but not in the simulations, will dominate the wavelet transform.

Finally, the Fourier approach is also applied to examples 6 and 7, and the results are also presented in Table 3. The damping is estimated by the 3-dB method [24]. Although the Fourier approach can obtain acceptable results (errors less than 10%), the results are not as good as those by the proposed method, as seen from Table 3. The estimation errors of natural frequencies by the proposed method are only 1/2 to 1/4 of those by the Fourier approach. Since actual damping ratio is unknown, no comparison can be made. However, it is believed that the proposed method can provide a much better estimation for damping. As mentioned at the beginning of Introduction, the Fourier approach cannot give good estimation for damping. Note that the Fourier approach here has used the denoised data. If the un-denoised data were used, the results can be worse. Moreover, it is obvious that the Fourier approach cannot be applied to example 2 (heavily damped system) and example 5 (strongly coupled modes), whereas the proposed method can still get good results.

6. Conclusions

In this study, the Morlet wavelet transform of the free or forced response has been utilized to identify the natural frequency and damping ratio of vibration systems. The method can be applied to both single- and multi-dof systems with the same level of accuracy, and it can be applied to lightly or heavily damped systems. The method is based on a relationship between the system parameters and the Morlet wavelet transform of the

system response. It is found that the validity of the relationship depends on the scaling factor a, translation factor b, and the frequency parameter ω_0 of the Morlet wavelet transform. Therefore, the identification accuracy depends also on a, b, and ω_0. Proper choice of a, b, and ω_0 is crucial for good identification results. A general guideline of choosing a, b, and ω_0 has been proposed in this paper.

Numerical simulations showed that all identification errors (for natural frequency and damping ratio) are less than 1% for lightly damped systems, 1-dof or 4-dof. For the heavily damped or strongly coupled system, the result for ω_n is still good (less than 1% in error). Although the result for ζ is not as good as those for lightly damped or lightly coupled systems, the estimation error can still be kept within 10%. Moreover, the experimental results showed that good identification accuracy (less than 3% in error) can still be obtained even for noisy 1-dof or multi-dof systems. These results clearly verify the theoretical analysis.

Acknowledgements

The authors would like to thank Mr. Keng-Chu Ho and Mr. Chang-Yen Chou for performing the numerical simulations. This work is partially supported by the National Science Council of Taiwan, ROC, under Grant NSC 90-2213-E-194-029.

Appendix A

This appendix is to prove Eq. (8). Let $\hat{\tau} = \tau + \alpha$. Then, it is easy to see that

$$\int_{-\infty}^{\infty} e^{(-1/2)(\tau+\alpha+j\beta)^2}\, d\tau = \int_{-\infty}^{\infty} e^{(-1/2)(\hat{\tau}+j\beta)^2}\, d\hat{\tau}$$

Consider now the contour integral

$$I = \oint_C e^{(-1/2)z^2}\, dz$$

where C is the rectangular contour shown in Fig. A1, which is composed of L_i, $i = 1$–4. Since $e^{-(1/2)z^2}$ is analytic inside C, $I = 0$, i.e.,

$$\int_{L_1} e^{(-1/2)z^2}\, dz + \int_{L_2} e^{(-1/2)z^2}\, dz + \int_{L_3} e^{(-1/2)z^2}\, dz + \int_{L_4} e^{(-1/2)z^2}\, dz = 0$$

It is easy to show that the integrals over L_2 and L_4 approach zero when $R \to \infty$. Also, when $R \to \infty$, we have

$$\int_{L_1} e^{(-1/2)z^2}\, dz = \int_{-\infty}^{\infty} e^{(-1/2)x^2}\, dx \quad \text{and} \quad \int_{L_3} e^{(-1/2)z^2}\, dz = -\int_{-\infty}^{\infty} e^{(-1/2)(x+i\beta)^2}\, dx$$

The former integral is well known to be $\sqrt{2\pi}$. Hence, we obtain Eq. (8).

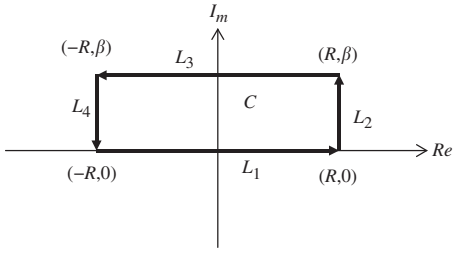

Fig. A1. The contour C.

References

[1] S.-L. Chen, H.-C. Lai, K.-C. Ho, Identification of linear time varying systems by Haar wavelets, *International Journal of System Science* 37 (9) (2006) 619–628.

[2] C.K. Chui, *An Introduction to Wavelets*, Academic Press, Boston, 1992.

[3] M.I. Doroslovacki, H. Fan, Wavelet-based linear system modeling and adaptive filtering, *IEEE Transactions on Signal Processing* 44 (5) (1996) 1156–1167.

[4] R. Ghanem, F. Romeo, A wavelet-based approach for the identification of linear time-varying dynamical systems, *Journal of Sound and Vibration* 234 (4) (2000) 555–576.

[5] R. Ghanem, F. Romeo, A wavelet-based approach for model and parameter identification of nonlinear systems, *International Journal of Nonlinear Mechanics* 36 (2001) 835–859.

[6] B. Jawerth, W. Sweldens, An overview of wavelet based multiresolution analysis, *Society for Industrial and Applied Mathematics* 36 (3) (1994) 377–412.

[7] R. Johansson, *System Modeling and Identification*, Prentice-Hall, Englewood Cliffs, NJ, 1993.

[8] T. Kijewski, A. Kareem, On the presence of end effects and associated remedies for wavelet-based analysis, *Journal of Sound and Vibration* 256 (5) (2002) 980–988.

[9] T. Kijewski, A. Kareem, Wavelet transforms for system identification in civil engineering, *Computer-Aided Civil and Infrastructure Engineering* 18 (5) (2003) 339–355.

[10] C.-H. Lamarque, S. Pernot, A. Cuer, Damping identification in multi-degree-of-freedom systems via a wavelet-logarithmic decrement—part 1: theory, *Journal of Sound and Vibration* 235 (3) (2000) 361–374.

[11] J. Lardies, S. Gouttebroze, Identification of modal parameters using the wavelet transform, *International Journal of Mechanical Science* 44 (11) (2002) 2263–2283.

[12] D.E. Newland, Wavelet analysis of vibration—part 1: theory, *ASME Journal of Vibration and Acoustics* 116 (1994) 409–416.

[13] D.E. Newland, Wavelet analysis of vibration—part 2: wavelet maps, *ASME Journal of Vibration and Acoustics* 116 (1994) 417–425.

[14] M. Pawlak, Z. Hasiewicz, Nonlinear system identification by the Haar multi-resolution analysis, *IEEE Transactions on Circuits and Systems I: Fundamental Theory and Applications* 45 (1998) 945–961.

[15] S. Palavajjhala, R.L. Motard, B. Joseph, Process identification using discrete wavelet transforms: design of prefilters, *AIChE Journal* 42 (3) (1996) 777–790.

[16] Z. Peng, F. Chu, P. Tse, Detection of the rubbing caused impacts for rotor–stator fault diagnosis using reassigned scalogram, *Journal of Mechanical Systems and Signal Processing* 19 (2) (2005) 391–409.

[17] R.D. Priebe, G.R. Wilson, Wavelet applications to structural analysis, *IEEE International Conference on Acoustics, Speech, and Signal Processing* 3 (1994) 205–208.

[18] A.N. Robertson, K.C. Park, K.F. Alvin, Identification of structural dynamics models using wavelet-generated impulse response data, *ASME Journal of Vibration and Acoustics* 120 (1998) 261–266.

[19] A.N. Robertson, K.C. Park, K.F. Alvin, Extraction of impulse response data via wavelet transform for structural system identification, *ASME Journal of Vibration and Acoustics* 120 (1998) 252–260.

[20] M. Ruzzene, A. Fasana, L. Garibaldi, B. Piombo, Natureal frequencies and dampings identification using wavelet transform: application to real data, *Mechanical Systems and Signal Processing* 11 (1997) 207–218.

[21] D.A. Schoenwald, System identification using a wavelet-based approach, *Proceedings of the 32nd IEEE Conference on Decision and Control*, Vol. 4, 1993, pp. 3064–3065.

[22] J. Slavic, I. Simonovski, M. Boltezar, Damping identification using continuous wavelet transform: application to real data, *Journal of sound and Vibration* 262 (2003) 291–307.

[23] W.J. Staszewski, J.E. Cooper, Flutter data analysis using the wavelet transform, *Proceedings of the MV2 International Congress on New Advances in Modal Synthesis of Large Structures: Nonlinear Damped and Non-Deterministic Cases*, Lyon, France, 5–6 October 1995, pp. 549–561.

[24] W.J. Staszewski, Identification of damping in MDOF systems using time-scale decomposition, *Journal of Sound and Vibration* 203 (2) (1997) 283–305.

[25] W.J. Staszewski, Identification of nonlinear systems using multi-scale ridges and skeletons of the wavelet transform, *Journal of Sound and Vibration* 214 (4) (1998) 639–658.

[26] W.J. Staszewski, J.E. Cooper, Wavelet approach to flutter data analysis, *AIAA Journal of Aircraft* 39 (1) (2002) 125–132.

[27] N. Sureshbabu, J.A. Farrell, Wavelet-based system identification for nonlinear control, *IEEE Transaction on Automatic Control* 44 (2) (1999) 412–417.

[28] M.K. Tsatsanis, G.B. Giannakis, Time-varying system identification and model validation using wavelets, *IEEE Transactions on Signal Processing* 41 (12) (1993) 3512–3523.

[29] B. Yan, A. Miyamoto, A comparative study of modal parameter identification based on wavelet and Hilbert–Huang transformation, *Computer-Aided Civil and Infrastructure Engineering* 21 (2006) 9–23.